Classification of UWB Multipath Clusters and Its Distortion Effects on Positioning Error

K. Makaratat, TWC. Brown, S. Stavrou, and B. Evans

Centre for Communication Systems Research, University of Surrey
Guildford, Surrey, GU2 7XH, United Kingdom

K.Makaratat@surrey.ac.uk, T.Brown@surrey.ac.uk, S.Stavrou@surrey.ac.uk, B.Evans@surrey.ac.uk

***Abstract*—Quantification of distortion effects on UWB system performances in terms of positioning error is analysed in this research. UWB multipath distorted channels are simulated in each frequency subband, over 2-11 GHz. Its characteristics are modelled corresponding to multipath clusters along the propagation paths. The classification of clusters and physics-based distortion mechanisms are generalized to be included into the simulation algorithm. Finally, distortion impacts on system performances regarding to frequency dependent characteristics and positioning errors are investigated.**

I. INTRODUCTION

Ultrawideband (UWB) pulse distortions are inherently characterised by the extremely large bandwidth. Since quantifying the impacts of pulse distortion on UWB system performance appears to be novel, recently there are several works reported about quantification of UWB distortion effects in addition to the physics-based pulse distortion issues which have been addressed in previous research [1]-[4]. Inter symbol interference (ISI) and probability of bit error rate (BER) due to distortion effects in various complex propagation conditions are commonly investigated as researched by [5]-[7]. Furthermore, Zhou [8] also reported loss of signal-to-noise ratio (SNR) as high as 4 dB in template mismatches due to distortion effects. Moreover, the much larger error range than the Cramer-Rao lower bound (CRLB) was found in this study. These lead to errors that can limit the accuracy of times-of-arrival (TOAs) of received multipath signals. The very high temporal resolution of UWB pulse signals makes UWB signals become the ideal candidates for combined communications and positioning. If the TOAs of incoming multipath signals are known with little uncertainty, the computation of propagating distances from the source to the receivers is still possible with a few errors in estimation. Yuan *et al*. reported the deterioration of UWB positioning performance due to distortions even though the modified phase-only correlator method for high-resolution multi-target ranging was employed [9].

Thus, the effect of UWB distortions becomes significant and should be investigated to quantify its impact on system performances and to examine the suitable methods for compensating its deteriorating effects. Consequently, this paper reports the quantification of frequency distortion in terms of positioning error. Characteristics of signal dispersion due to various multipath distortion conditions are analysed. Distortion and positioning errors in individual multipath components subject to specific scenarios and obstruction materials are analysed herein.

II. CLASSIFICATION OF UWB MULTIPATH CLUSTERS

According to multipath cluster investigations derived from many indoor UWB measurements [10]-[14], each multipath cluster could be identified by a group of MPCs, which are scattered or reflected from obstructions, with similar angles-of-arrival (AOAs), angles-of-departure (AODs), and TOAs. The received multipath clusters from dominant propagation paths from a transmitter to a receiver are expected to come from three types of radio propagation paths. The first group corresponds to scattering nearby the transmitter site. Similarly, another group of clusters can be observed at the receiver site due to the scattering objects in the neighbouring area of the receiver. Finally, line-of-sight (LOS) components between the transmitter and the receiver are considered. Consequently, these different propagation clusters can be classified into three classes as Class-I, Class-II and Class-III type of clusters respectively [15] as illustrated in Fig. 1 where the omnidirectional antenna is considered as the transmitter, and 3x3 planar array antenna is the receiver.

When defining significant clusters specifically related to propagation scenarios, in the LOS scenario of Case-A describing a small furnished office room, the channel would be dominated by Class-III clusters. Next, the non-line-of-sight (NLOS) scenario Case-B is considered where a transmitter and a receiver are in the same office room with a-light-wall or a-cloth-partition separation between both ends; the channel would be still dominated by Class-III clusters. However, when propagation paths in a larger furnished office room, NLOS scenario Case-C, are considered, all three classes of clusters are presented. Finally, if a transmitter and a receiver are located in a different furnished room or separated by a thick wall, the channel would be dominated by Class-I and Class-II clusters corresponding to the extreme NLOS condition (Case-D). Diagrams of four channel propagation cases corresponding to cluster classifications are depicted in Fig. 1 (a)-(d) for LOS Case-A, NLOS Case-B, NLOS Case-C, and NLOS Case-D respectively. All individual multipath components (MPCs) are taken into account corresponding to dominated clusters and specific environments.

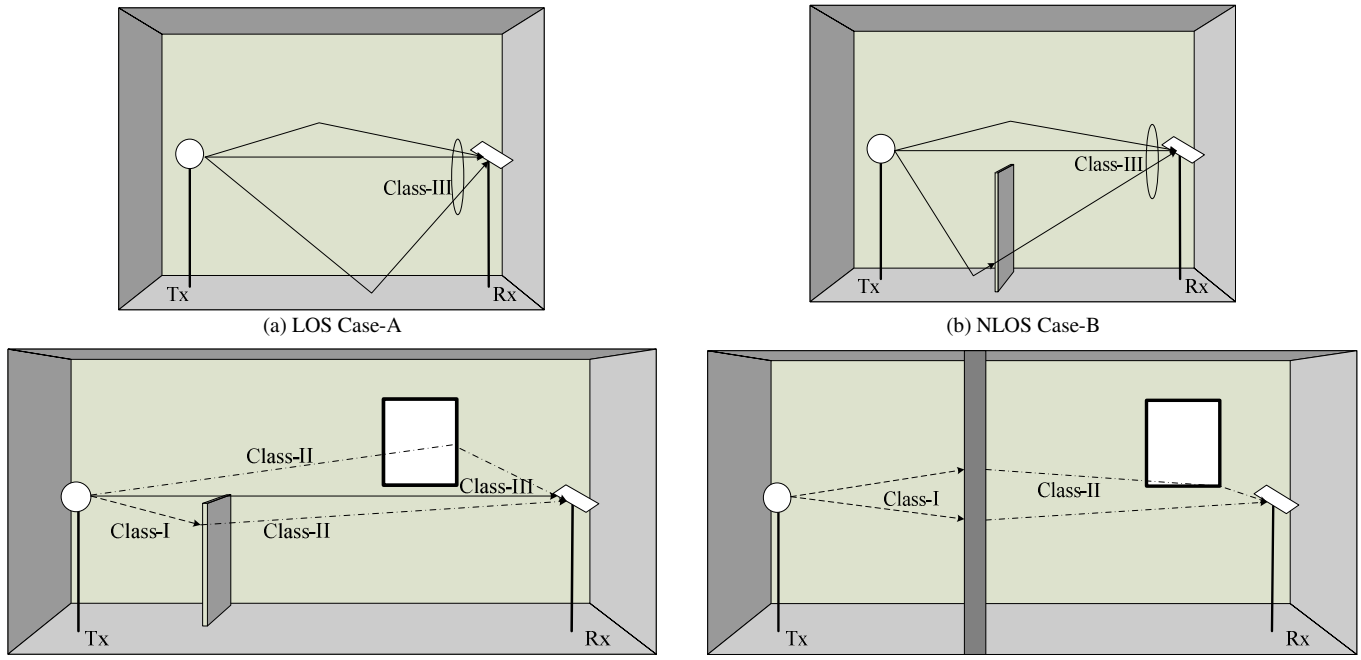

(a) LOS Case-A (b) NLOS Case-B

(c) NLOS Case-C (d) NLOS Case-D

Fig. 1 Configuration of UWB multipath clusters in indoor environments

Consequently, in order to construct realistic UWB propagation channels, classified MPC clusters and pulse distortion effects are simulated together. Typically, the total response, $h(\tau)$, from a complex multipath channel can be modeled by the summation of all impulse responses of local scattering with the closed form expression of specific geometric configurations. Unlike typical UWB channel models, this simulation relies on combining pulse distortion characteristics into the UWB channel impulse response (CIR) model. Frequency-dependent effects are included into the simulation as each CIR model is considered at each frequency subband, s, [7], [18]. According to Fig. 1, in the LOS scenario of Case-A, the channel would be dominated by Class-III clusters and distorted by multiple reflections and half-plane diffraction as defined by

$$h_{case-A}(s,\tau,\theta,\phi) = h^{III}_{LOS}(s,\tau,\theta,\phi) + h^{III}_{GO}(s,\tau,\theta,\phi) + h^{III}_{half-plane}(s,\tau,\theta,\phi) \quad (1)$$

Next, the channel in the NLOS Case-B would be still dominated by Class- III clusters and distorted by the similar effects as Case-A. However, thin slab diffraction is additionally included into the distortion model, $h^{III}_{thin-slab}(s,\tau,\theta,\phi)$ to construct h_{case-B}. When UWB signals propagating in a larger furnished office room, NLOS Case-C, all three classes of clusters are presented. All distortion effects might possibly appear in Class-III similarly to LOS-A, but distortions due to thin slab diffraction and thick slab reflection are modeled for Class-II clusters. CIRs of Case-C can be described by (2) where $g^I(s,\theta_{Tx},\sigma_{Tx})$ is the single-directional CIR of Class-I clusters at the transmitter site. θ_{Tx} and ϕ_{Tx} are the elevation and azimuth AOD of the MPCs.

$$h_{case-C}(s,\tau,\theta,\phi) = h^{III}_{GO}(s,\tau,\theta,\phi) + h^{III}_{half-plane}(s,\tau,\theta,\phi) + h^{II}_{thin-slab}(s,\tau,\theta,\phi) + h^{II}_{thick-slab}(s,\tau,\theta,\phi) + g^{I}(s,\theta_{Tx},\phi_{Tx}) \quad (2)$$

Finally, in the severest NLOS Case-D, the channel would be dominated by Class-I and Class-II clusters corresponding to room separation by a thick wall. Only thick slab reflection is considered. Thus only the last two terms in (2) are taken into account for this h_{case-D}. All technical terms of h_{LOS}, h_{GO}, $h_{half-plane}$, $h_{thin-slab}$, and $h_{thick-slab}$ are not illustrated in this paper, but their formulas are written in detail as defined in [1] and [4].

III. Positioning Error

In addition to SNR loss and BER due to the pulse shape mismatch, pulse distortion can also degrade synchronisation and positioning by time shifting of TOAs as well as an amplitude error in the correlation peak. Basically, the accuracy of the TOA estimation or positioning errors caused by pulse distortion is expressed by the minimum variance of the TOA estimation error, σ^2_τ in terms of the CRLB. This value is related to signal bandwidths and SNR at the receiver. For a single path additive white Gaussian noise (AWGN) channel, the best achievable accuracy of a position estimate, which is derived from TOA estimation, satisfies the following inequality [16], [17]:

$$\sqrt{\sigma_\tau^2(d)} \geq \frac{c}{2\sqrt{2}\pi\beta\sqrt{SNR}} \quad (3)$$

This value benchmarks the positioning error caused by pulse distortion. Thus, the minimum estimated position error less than d_{CRLB} m can be obtained when considering SNR=0. c= 3x10^8 m/s and β is the effective or root mean square signal bandwidth given by function of the Fourier transform of the transmitted signal, $P(f)$. In this study, frequency domain of pulse position modulation time hopping (PPM-TH-UWB) transmitted signals is considered to compute β over 2-11 GHz.

$$\beta \approx \left[\int_{-\infty}^{\infty} f^2 |P(f)|^2 df \Big/ \int_{-\infty}^{\infty} |P(f)|^2 df \right]^{1/2} \quad (4)$$

In this work, PPM-TH-UWB is generated as the transmitted signal, $W(\tau)$, and transmitted over the synthesised classified multipath channels; therefore channel impulse responses including cluster types and distortion effects [1], [4] are taken into account to quantify distortion impacts. Results of this research are described in the next section.

IV. QUANTIFICATION RESULTS OF DISTORTION EFFECTS

Binary PPM-TH-UWB is generated as the transmitted signal conveying 3000 bits through 3000 pulses, thus code repetition coding is not applied. The average pulse repetition period is 60ns guaranteeing the absence of inter symbol interference (ISI) in LOS. These generated signals, $W(\tau)$, are simulated and transmitted over the synthesized multipath channels as specifically classified in each environment; therefore channel impulse responses (CIRs), $h(\tau)$, including cluster types and distortion effects are taken into account. Positioning errors due to pulse distortion are computed and shown in Table 1 regarding classification of scenario cases, cluster types and obstruction materials. In order to present the pulse distortion effects on UWB propagation channels, comparison between lower bound average distance estimation errors computed by CRLB and estimated ranging errors are described. Since β, 3.4 GHz, is calculated from the same transmitted signals over 2-11 GHz, all scenario cases take into account the same value of β leading to the lower bound distance error of d_{CRLB}=0.99 mm. in all scenario cases.

Ranging errors are examined by time difference of correlation peaks between pulse signals as depicted in Fig. 2. Fig. 2 (a) presents the ideal case of free space LOS scenario where autocorrelation results of the received pulse $R(\tau)$ shown by the solid line and autocorrelation results of the transmitted pulse $W(\tau)$, the dashed line, present the same peaks of the waveforms. Both peaks of these symmetric waveforms correctly indicate the position. Since the impact of pulse distortion is examined in this study, $W(\tau)$ is considered as the local template to be correlated with the received distorted signals $R(\tau)$ as shown in Fig. 2 (b)-(f). The solid line presents the correlation result between different templates, $W(\tau)$ and $R(\tau)$. These two different templates are normalised to have the same energy before correlating. Moreover, the dashed curve is the result of correlation with the same template itself or autocorrelation of $W(\tau)$. The symmetric autocorrelation waveform can be observed contrary to the different template correlation whose the asymmetric waveform gives an error in

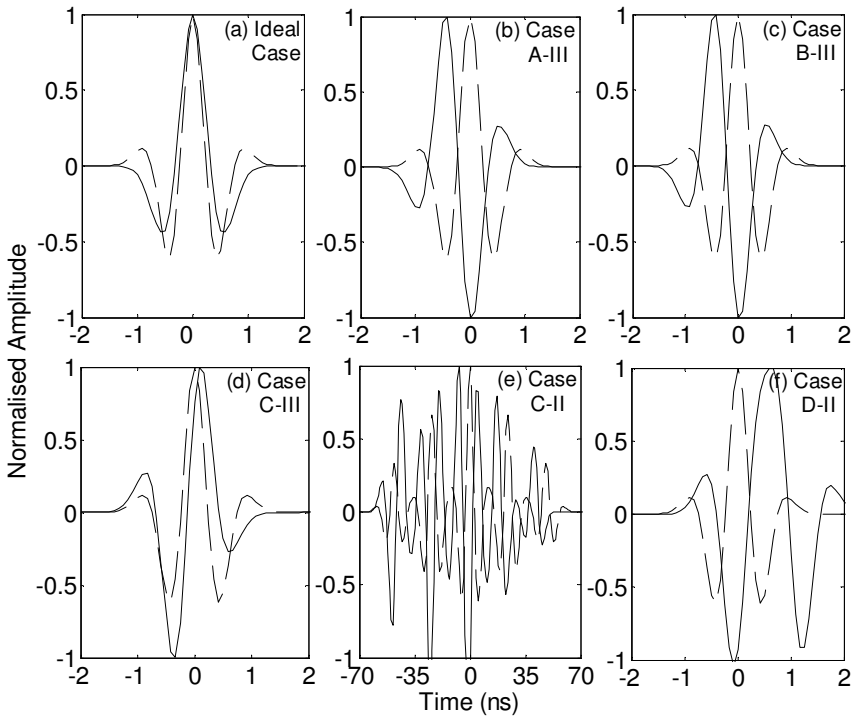

Fig. 2 Correlation of distorted signals with transmitted signals

TABLE 1
PULSE DISTORTION IMPACTS ON POSITIONING ERROR

Distortion Channels	Obstruction Material	RMS Bandwidth β (GHz)	d_{CRLB} (mm) at SNR=0	Centre Frequency Subband, f_c (GHz)	Order of MPCs	Timing Error (ns)	Ranging Error (mm)
LOS Case A-III	Wallboard	3.4	0.99	4	1	0.083	24.9
					2	-0.415	-124.5
NLOS Case B-III	Wallboard	3.4	0.99	9	1	0.083	24.9
					2	-0.418	-125.4
					3	-0.333	-99
					4	-0.50	-150
NLOS Case C-III	Wooden door	3.4	0.99	4	1	-0.083	-24.9
					2	0.083	24.9
					3	0.333	99
NLOS Case C-II	Partition	3.4	0.99	6	4	-0.417	-125.1
	Concrete Block				5	-0.584	-175.2
NLOS Case D-II	Concrete Block	3.4	0.99	10	1	0.584	175.2
					2	0.583	174.9
					3	0.083	24.9
					4	0.167	50.1

the position. Distinguishing the difference between these two peaks can define timing errors as also shown in Table 1.

Negative values of timing errors refer to position shifting prior to the reference time, which is indicated by the symmetric waveform peak. When multiplying timing errors by the light velocity, c=3x10^8, ranging errors can be defined. Comparing ranging error distances and the lower bound distance error, d_{CRLB}=0.99 mm, results significantly show that apart from SNR, distortion effect can cause performance degradation in positioning errors much bigger than d_{CRLB}. The second MPCs scattered from obstruction clusters class-III in scenarios Case-A, Case-B and Case-C are examined as illustrated in Fig. 2 (b)-(d) respectively. Since a few difference in timing errors is rarely observed in the first MPCs corresponding to LOS components or the-shortest-distance propagation paths, to present noticeable timing error characteristics caused by distortion, the later components of multipath receiving pulses are selected as examples to be shown. The fifth and the fourth MPCs originated from clusters class-II in scenarios Case-C and Case-D are also presented in figure (e) and (f) respectively.

These examples of received pulse distortion are analysed specifically at the highest energy allocation frequency subbands, as stated in [7] and [18], with various types of obstruction material. Timing errors of propagation channels in Case C-III are less than in Case-A and Case-B notwithstanding its propagation through various obstructions along the path. This might be due to these pulse distortion effects are selected as examples taken into account different frequency subbands and different obstruction. Figure (e) presents the correlation of dense multipath channels of Case-C propagation. The later fifth MPC scattered by concrete block obstruction, cluster Class-II, gives the highest timing error of -0.584 ns or the ranging error of -175.2 mm. And 0.167 ns timing error or 50.1 mm. ranging error can be seen for the fourth MPC of Case D-II due to thick slab reflection from concrete block.

Furthermore, comparison of pulse distortion effects on each MPC at each propagation channel is also presented in Table 1. Generally, positioning errors of the first three MPCs in propagation channels obstructed by cluster Class-III are roughly in the same range and less than errors caused by cluster Class-II. More errors are remarkably estimated in later MPCs of propagation Case C-II. Moreover, low values of positioning errors in Case D-II in the fourth and the fifth MPCs are irregularly observed. This can be assumed that amplitudes of received MPCs are considerably attenuated along propagation paths without extremely distorted pulse shape, hence correlating normalised received pulses, the 4th and 5th MPCs, with the local template $W(\tau)$ possibly gain small timing and ranging errors.

V. CONCLUSIONS

Significant results of the frequency-dependent characteristics and the quantification of distortion effects on UWB multipath channels were presented. Apart from the probability of bit error rate, performance degradation in

positioning errors was determined to quantify distortion effects on UWB multipath channels for all frequency subbands. Correlation between distorted pulses and transmitted pulses determined timing and ranging errors which these positioning errors extremely exceeded the benchmark errors estimated by CRLB. In addition, results also examined that LOS component gained more accuracy of positioning errors than late-arrival NLOS distorted components

REFERENCES

[1] R. C. Qiu, "A generalized time domain multipath channel and its application in ultra-wideband (UWB) wireless optimal receiver – part II: physics-based system analysis," *IEEE Trans Wireless Commun*., vol. 3, no. 6, pp. 2312-2324, Nov. 2004.

[2] G. Wang, and W. Kong, "Angle-dependent pulse distortion in UWB radiation and its impact on UWB impulse communications," *Electronics Letters*, vol. 41, no. 25, pp. 1360 – 1362, Dec. 2005.

[3] A. Muqaibel, A. Safaai-Jazi, A. Bayram, A.M. Attiya, and S. M. Riad, "Ultrawideband through-the-wall propagation," *IEE Proc. Microw. Antennas Propag.*, vol. 52, no. 6, pp. 581- 588, Dec. 2005.

[4] R. C. Qiu, "A generalized time domain multipath channel and its application in ultra-wideband (UWB) wireless optimal receiver – part III: system performance analysis," *IEEE Trans Wireless Commun*., vol. 5, no. 10, pp. 2685-2695, Oct. 2006.

[5] M. Z. Win, and R. A. Scholtz, "Characterization of ultra-wide bandwidth wireless indoor channels: a communication-theoretic view," *IEEE J. Sel. Areas. Commun*., vol. 20, pp. 1613-1627, 2002.

[6] Y. Zhang, and A. K. Brown, "Complex multipath effects in UWB communication channels," *Proc. IEE Commun*., vol. 153, no. 1, pp. 120-126, Feb. 2006.

[7] K. Makaratat, T.W.C. Brown, and S. Stavrou, "Modified UWB spatio-temporal channel simulation including pulse distortion and frequency dependence," *IEEE Antennas and Wireless Propag. Lett*., vol. 7, pp. 552-555, 2008.

[8] Z. Chenming, and R. C. Qiu, "Pulse Distortion Caused by Cylinder Diffraction and Its Impact on UWB Communications," *IEEE Trans. Veh. Technol.*, vol. 56, no. 4, pp. 2385-2391, Jul., 2007.

[9] Z. Yuan, C. L. Law, L. G. Yong, and F. Chin, "Multi-target UWB passive ranging with local template uncertainty," in *IEEE Proc. Int. Conf. on Ultra-Wideband, 2008* (ICUWB 2008), Hannover, Germany, Sep. 2008, pp. 233-236.

[10] A. Saleh and R. A. Valenzuela, "A statistical model for indoor multipath propagation," *IEEE J. Sel. Areas Commun.*, vol. 5, no. 2, pp. 128–137, Feb. 1987.

[11] C. Chong, Y. Kim, and S. S. Lee, "A modified S-V clustering channel model for the UWB indoor residential environment," in *IEEE Proc.* on *Vehicular Technology Conference 2005*, Stockholm, Sweden, May 2005, pp 58-62.

[12] Q. H. Spencer, B. D. Jeffs, M. A. Jenson, and A. L. Swindlehurst, "Modeling the statistical time and angle of arrival characteristics of an indoor multipath channel," *IEEE J. Sel. Areas. Commun.*, vol. 18, no.3, pp. 347- 359, Mar. 2000.

[13] K. Haneda, J. Takada, and T. Kobayashi, "Cluster properties investigated from a series of ultrawideband double directional propagation measurements in home environments," *IEEE Trans. Antennas Propag.*, vol. 54, no. 12, pp. 3778- 3788, Dec. 2006.

[14] R. J. M. Cramer, R. A. Scholtz, and M. Z. Win, "Evaluation of an ultra-wide-band propagation channel," *IEEE Antennas Propag.*, vol. 50, no. 5, pp. 561- 570, May. 2002.

[15] Y. Chen and V. K. Dubey, "Dynamic simulation model of indoor wideband directional channels," *IEEE Trans. Veh. Technol.*, vol. 55, no. 2, pp. 417- 430, Mar. 2006.

[16] S. Gezici, A. Tian, G. B. Giannakis, H. Kobayashi, A. F. Molisch, H. V. Poor, and A. Sahinoglu, "Location via ultra-wideband radios," *IEEE Signal Process. Mag.*, vol. 22, pp. 70-84, Jul. 2005.

[17] H. Urkowitz, Signal Theory and Random Processes. Dedham, MA: Artech House, 1983.

[18] K. Makaratat, S. Stavrou, and T.W.C Brown, "Simulation of UWB distortion combined with indoor spatio-temporal channels," in *Proc. IET Seminar* on *Wideband and Ultrawideband Systems and Technologies*, London, 6 Nov. 2008.